Measuring nanomechanical properties of a dynamic contact using an indenter probe and quartz crystal microbalance

B. Borovsky[a)] and J. Krim[b)]
Department of Physics, Box 8202, North Carolina State University, Raleigh, North Carolina 27695-8202

S. A. Syed Asif[c)] and K. J. Wahl
Code 6170, Chemistry Division, Naval Research Laboratory, Washington, DC 20375-5342

A study of the contact mechanics of a probe tip interacting with a quartz crystal microbalance (QCM) has been performed, involving simultaneous measurements of normal load, displacement, and contact stiffness with changes in QCM resonant frequency. For metal–metal and glass–metal contacts in air, the QCM frequency shifts were observed to be positive, and directly proportional to the contact area as inferred from the contact stiffness. Interfacial characteristics of the probe–tip contact (elasticity, contact size, and an estimate of the number of contacting asperities) were deduced by extending a prior model of single asperity contact to the case of multiple contacts. The extended model clarifies a number of seemingly disparate experimental results that have been reported in the literature. © *2001 American Institute of Physics.* [DOI: 10.1063/1.1413493]

I. INTRODUCTION

Knowledge of the physical properties of small contacting asperities is a topic that is of increasing importance to a number of macroscopic and microscopic applications. Numerous experimental characterizations of the physical properties of nanoscale contacts have been performed by means of nanoindentation,[1–4] atomic force microscopy[5–8] and scanning tunneling microscopy (STM).[9,10] More recently, it has become recognized that a probe tip-quartz crystal microbalance (QCM)[11–20] or closely related geometries[21] could also have enormous potential as a sensitive probe of interfacial physical properties. The principle underlying such experiments is that the extremely sharp resonance of a quartz crystal is sensitive to interaction forces applied to its surfaces. Changes in resonance frequency f_0 and quality factor Q reflect the additional energy storage and loss accompanying the interaction. In general, all four combinations of increasing or decreasing f_0 and increasing or decreasing Q are possible.[22] Beginning in 1994, the frequency shift of a QCM in response to a contacting probe tip was reported by groups independently seeking to characterize asperity contacts. Krim and co-workers[11,12] reported negative frequency shifts and decreases in Q due to the presence of a STM tip for adsorbed water films of varying thickness. Sasaki *et al.*[13,14] reported the use of STM for "scanning shear stress microscopy," attributing the observed QCM frequency shifts to be directly proportional to interfacial shear stress. The spatial contrast in these and similar experiments[15,16] has been variously attributed to local friction, elasticity, or viscoelasticity.

Two groups have recently evaluated the QCM–probe interaction to interpret the physical properties of such contacts.

Laschitsch and Johannsmann[17–19] (LJ) studied a number of materials combinations and reported positive frequency shifts and decreased quality factors. They presented a model, assuming a single asperity contact, which predicted positive frequency shifts linearly proportional to contact radius. In contrast, Flanigan *et al.*[20] directly measured the contact area between a QCM and a polymer gel cap and observed a negative frequency shift directly proportional to the contact area. A model based on known expressions for the QCM frequency shift on full immersion in a fluid medium was used to deduce the viscoelastic properties of the gels.

The seemingly disparate results reported in the literature stem largely from the fact that no experimental group has performed measurements in completely characterized situations (normal force, contact area, etc.), and thus untested assumptions have necessarily been incorporated into the analyses. In order to simultaneously measure the relevant physical parameters to interpret such measurements, we have used a combined nanoindenter-QCM apparatus. This allows independent measurement of the applied load, normal displacement, and contact stiffness, while simultaneously monitoring the frequency shift of the QCM. The advantage of measuring the displacement and contact stiffness throughout the QCM–probe interaction is that it allows quantitative evaluation of the contact mechanics governing the interaction. For the probe and surface configuration employed in our experiments, we observed that the frequency shift of the QCM was positive and linearly proportional to the contact area. Interfacial characteristics of the probe–tip contact (elasticity, contact size, and an estimate of the number of contacting asperities) were deduced by extending the LJ model of single asperity contact to the case of multiple contacts. The extended model clarifies a number of the experimental results that have been reported in the literature.

[a)]Present affiliation: Physics Department, Grinnell College, Grinnell, IA 50112.
[b)]Electronic mail: jkrim@unity.ncsu.edu
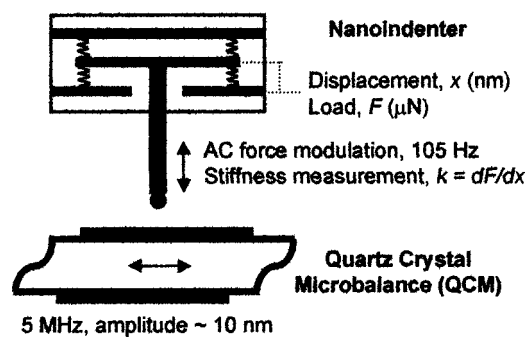[c)]Present affiliation: Hysitron Inc., Minneapolis, MN 55439.

FIG. 1. Schematic diagram of the experimental apparatus.

FIG. 2. Plot of QCM frequency shift vs normal load for contacts with the silica sphere (0.5 mm radius of curvature) and W tip (radius ~12 μm).
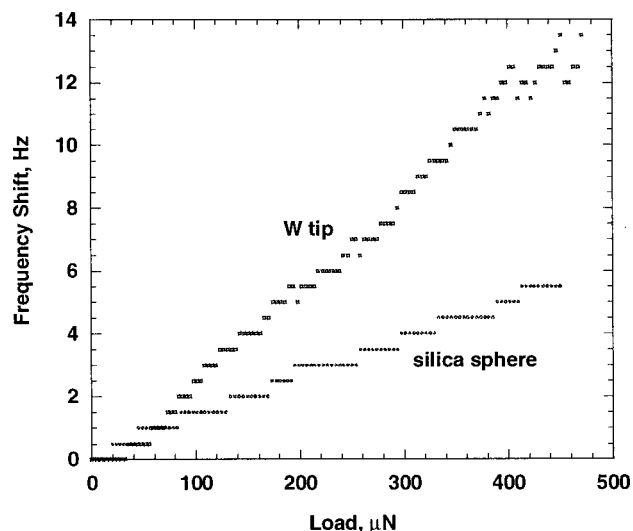
II. EXPERIMENT

Figure 1 shows a diagram of the experimental setup combining a depth-sensing nanoindenter and a QCM. The nanoindenter consists of a load-displacement transducer with electrostatic force actuation and displacement sensing electronics (Hysitron, Inc., Minneapolis, MN). With a custom force modulation setup,[23] this instrument enables dynamic measurements (at about 105 Hz in these experiments) of the contact stiffness normal to the substrate, K_n, and avoids problems associated with thermal drift. It is well established that for a spherical indenter tip, K_n is directly proportional to the contact radius, a_c, and given by

$$K_n = 2E^* a_c, \tag{1}$$

where E^* is the reduced Young's modulus.[24] With known reduced modulus of the materials in contact, the contact radius or area can be directly calculated from the measured contact stiffness.[2]

The QCM was clamped in a holder that secures the crystal at three points along its edge and mounted on an XYZ piezoscanner base (Digital Instruments, Santa Barbara, CA). The crystals used were fundamental mode 5 MHz AT (transverse shear mode)-cut circular quartz blanks with 1 cm diameter. Silver electrodes ~100 nm thick and 0.6 cm in diameter were thermally evaporated onto the blanks. The crystals were driven with a Clapp feedback oscillator circuit,[25] and the resonant frequency and amplitude[26] were monitored with a frequency counter and an oscilloscope, respectively. The quality factors of the resonators were measured with a simple ''ring-down'' technique[27] and were near 10^5. Two probes were used, a fused silica sphere (Duke Scientific, Palo Alto, CA), 0.5 mm radius, and an etched tungsten wire, ~12 μm tip radius. The experiments were conducted at atmospheric pressure in a dry nitrogen environment with 1%–10% relative humidity.

During a typical experiment, the QCM was first brought into contact with the indenter tip (~1 μN load setpoint) using the piezoscanner. Care was taken to center the indenter tip on the QCM electrode to maximize QCM sensitivity. Then, a preprogrammed indentation cycle (load/unload) was initiated. The normal force was ramped in either a staircase fashion with plateaus lasting 30 s, or with a linear ramp at loading rates of 25 to 50 μN/s with a 10–15 s hold before unloading; maximum loads were 100 to 500 μN. The data acquisition program simultaneously recorded the normal load, displacement of the probe, contact stiffness, and QCM resonant frequency. For the staircase ramp experiments, the resolution of the frequency shift was ±0.02 ppm (±0.1 Hz), using a gate time of 1 s. For the linear ramps, a faster gate time of 0.1 s was used, which reduced the frequency shift resolution to 0.5 Hz. The attractive forces during the initial contact of these probe tips with the QCM surface were insufficient to cause observable frequency shifts, as measured using a force–distance curve approach method.[28] In these experiments, a minimum load of approximately 5 μN was needed to observe a +0.1 Hz frequency shift with the 12 μm W tip.

III. EXPERIMENTAL RESULTS

Figure 2 shows an example of normal load versus QCM frequency shift for both the W tip and silica sphere contacts. The frequency response of the QCM was linearly proportional to applied load over a range up to 500 μN. For these contacts, loads of 30–50 μN were needed to obtain a 1 Hz frequency shift on the QCM. Figure 3 shows normal load versus contact stiffness data for the silica sphere. The response is clearly nonlinear, and is best fit with a square-root dependency. Deviation at the higher loads is the result of error in the measurement from a decrease in displacement amplitude with increasing contact stiffness. Similar behavior was observed for the contacts made using the W tip (not shown), which were also best fit with a square-root dependency.

The contact area can be estimated from the contact stiffness measurements using Eq. (1). The reduced modulus is given by

$$E^* = \left(\frac{1 - \nu_1^2}{E_1} + \frac{1 - \nu_2^2}{E_2} \right)^{-1}, \tag{2}$$

where E_i and ν_i are the Young's modulus and Poisson's ratios for the substrate and the probe. In calculating the reduced modulus, we have taken the thin Ag film on quartz as a single system with modulus 70 GPa and Poisson's ratio
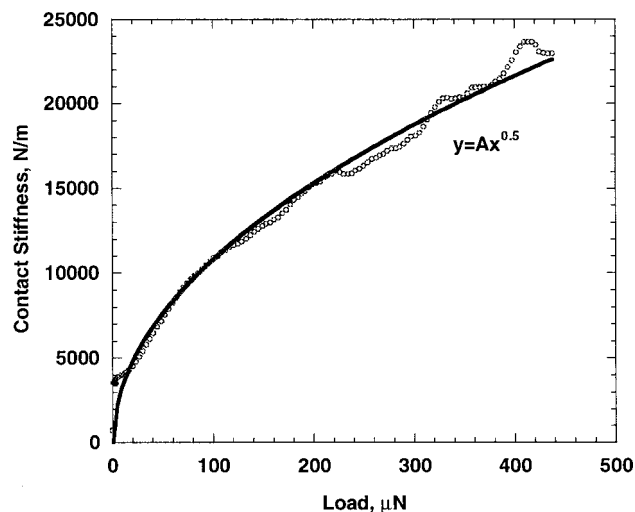
FIG. 3. Contact stiffness vs normal load for the silica sphere. The response is best fit with a square-root dependency.

FIG. 5. Frequency shift vs contact area for the silica sphere and *W* tip during loading to 500 μN.

0.2.[29] We assumed a modulus of 70 GPa and 345 GPa and Poisson's ratio of 0.2 and 0.28, for the silica sphere and W tip, respectively.[30] The resulting reduced moduli were 36 GPa for the silica sphere and 61 GPa for the *W* tip.

Figure 4 shows a plot of the calculated contact area versus normal load for both the silica sphere and W tip. Linear fits are shown, with R^2 values of 0.99. The linear relationship between contact area and normal load demonstrates that the contact is non-Hertzian. [For a sphere against flat geometry in Hertzian (elastic) contact, the contact area varies with load as $L^{2/3}$.] The linear relationship is however consistent with an interface that is multicontact and/or undergoing plastic deformation. Either of these conditions alone is sufficient to give the observed proportionality;[31] and both are expected to play a role. Load-displacement data (not shown) from indentations on the silvered region of the QCM showed evidence of plastic deformation under these loading conditions. Furthermore, the contact areas reported here always span a range much larger than the observed asperities on the QCM electrode surface,[32] so multicontact interfaces are expected.
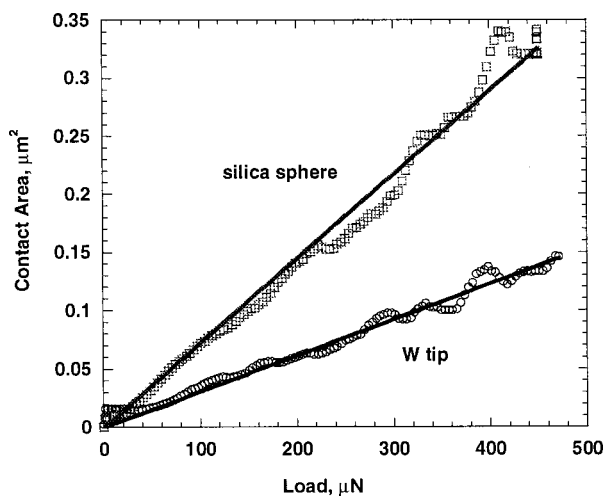
Figure 5 shows a plot comparing QCM frequency shift versus the contact area for both the W and silica contacts during loading to 500 μN. For both contacts, the relationship is linear (R^2 values 0.98–0.99), with a slope unique to each interface. (We note that departures from the linear relationship of Fig. 5 were sometimes observed for higher loads, indicating that the contact may be entering a new regime of deformation and/or wear.)

The linear relationship between frequency shift and contact area shown in Fig. 5 is an apparent contradiction with the LJ[17] model, which predicts a linear proportionality between frequency shift and contact radius. On the other hand, the linear relationship between contact area and frequency shift is consistent with the results of Flanigan *et al.*,[20] but the frequency shift is in the opposite direction. We propose that the multicontact nature of many probe–QCM interfaces is an important consideration. We now show that our results can be accounted for by modifying the LJ model accordingly. In doing so, the proportionality constants apparent in Fig. 5 may be analyzed in terms of the number and size of contacts at the interface.

IV. MODELING

In an earlier article, LJ considered a geometry in which the radius of the contact zone was much smaller than the wavelength of shear waves propagating into the probe.[17] In this model, the frequency shift Δf and "loss tangent" $\Delta \Gamma / \Delta f$ are each linearly proportional to the contact radius and can be identified with an "added stiffness" term. (Here, Γ is the half bandwidth at half maximum power). However, the derived proportionality between resonance shifts and contact radius could not be verified, as this required an explicit measurement of the contact size and its dependence on experimental parameters. The shear stress acting at the probe–QCM interface can be characterized using a wave model for the propagation of acoustic waves from the QCM into the probe. LJ employed this approach to derive the

FIG. 4. Contact area vs normal load calculated from the contact stiffness data during loading for the silica sphere and *W* tip.

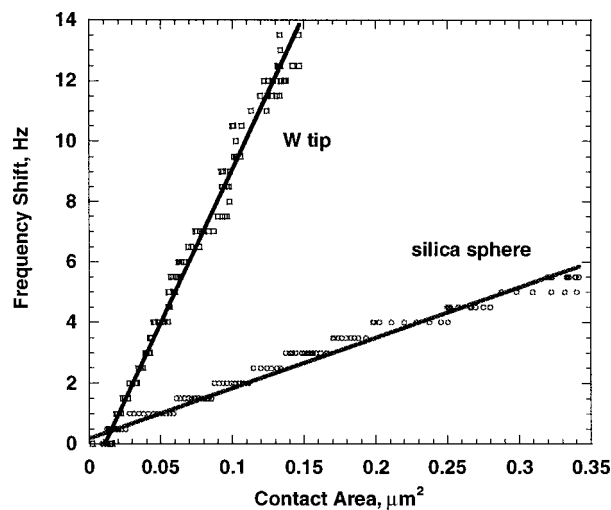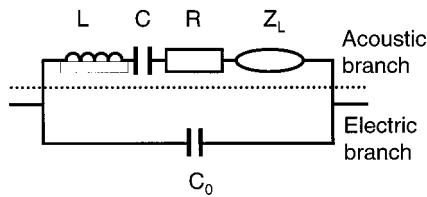FIG. 6. The BVD equivalent circuit for a QCM, with a small perturbing load impedance Z_L. L is proportional to the mass per unit area of the quartz blank, $1/C$ is proportional to the stiffness per unit area G/d (where G is the shear modulus and d the thickness of the quartz), and R is proportional to the viscous dissipation inside the quartz blank.

changes in QCM resonance parameters using a well-known equivalent circuit technique, which we briefly describe in the following paragraph.

Within linear circuit analysis, a QCM can be described as a damped harmonic oscillator by the lumped-element Butterworth–van Dyke (BVD) equivalent circuit, shown in Fig. 6. The BVD circuit is derived from the more rigorous transmission line model due to Mason with several reasonable approximations.[33] To be treated in this context, acoustic interactions involving the probe and quartz crystal are assumed to be both linear in displacement and one-dimensional, i.e., the acoustic waves are planar with no lateral variations.[34] The latter assumption is certainly not true in practice since the shear mode amplitude of a QCM decays in a Gaussian manner from the center of the electrode outwards,[35] and the interaction with the probe tip is very localized. (Normalization to the electrode active area introduced later on allows this otherwise one-dimensional model to account for much of the lateral variation.) Nevertheless, we state these assumptions and indicate that their limits of applicability must be tested.

The acoustic interaction between the probe and QCM was treated by LJ as an added load impedance Z_L in series with the other elements of the acoustic branch. For semi-infinite media, Z_L is simply the mechanical impedance evaluated at the interacting surface of the QCM. The mechanical impedance is defined by

$$Z_L = \sigma/v, \qquad (3)$$

where σ is the applied shear stress and v is the surface velocity. Z_L is a complex quantity and must be normalized to the electrode area. Since the changes in resonance parameters are only a few parts per million, the interaction between the probe and QCM can be treated as a small perturbation. Within the BVD damped harmonic oscillator model, the changes in resonant frequency and half bandwidth are given, to first order, by:

$$\Delta f = -\frac{f_0}{\pi} \frac{\text{Im}[Z_L]}{Z_q}, \qquad (4)$$

and

$$\Delta \Gamma = \frac{f_0}{\pi} \frac{\text{Re}[Z_L]}{Z_q}, \qquad (5)$$

where f_0 is the fundamental frequency and $Z_q = 8.8 \times 10^6$ kg m^{-2} s^{-1} is the acoustic impedance of AT-cut
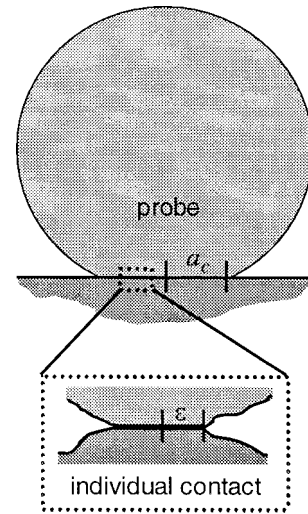

FIG. 7. Schematic diagram of the probe–QCM interface.

quartz. Notice that the loss tangent $\Delta\Gamma/\Delta f$ is simply the negative ratio of the real and imaginary parts of Z_L. For light damping, the change in dissipation D is given by

$$\Delta D = \Delta\left(\frac{1}{Q}\right) = \Delta\left(\frac{\Delta E}{2\pi E}\right) = \left(\frac{2\Delta\Gamma}{f_0}\right), \qquad (6)$$

where ΔE is the energy dissipated per cycle and E is the energy stored in the system.

To evaluate the mechanical impedance and determine the change in resonance parameters, one must propose an acoustic model and calculate the shear stress at the interface. We can show that a "near-field" acoustic geometry applies to our system, similar to that described by LJ. The wavelength of 5 MHz acoustic waves in all materials used here is near 600 μm,[36] whereas the contact radii are between 50 and 300 nm. Therefore, the contact radius is at least three orders of magnitude smaller than the wavelength of sound. As such, we expect sound to radiate into the tip as spherical waves decaying as ϵ/r, where ϵ is a characteristic size of the true contact regions (asperities) through which sound propagates, and r is the radial distance from the contact. The simplest way to represent the acoustic deformation of the contact is

$$u(r,t) = u_0 \frac{\epsilon}{r+\epsilon} e^{i(\omega t - kr)}, \qquad (7)$$

where u_0 is the amplitude of the QCM shear oscillation, ω is the angular frequency, and k is the wave number. As shown in Fig. 7, ϵ equals the contact radius a_c for a single-contact interface where the number of contacts $N = 1$.

For a multicontact interface, we propose ϵ is approximately constant as both N and the contact area increase in proportion to the load.[37] In this case, ϵ is determined by the nature of the roughness on the scale of the contact zone. Evaluating the shear stress at the interface, $r = 0$, we find:

$$\sigma \sim -K \frac{\partial u}{\partial r}\bigg|_{r=0} \sim -Ku_0\left(-\frac{1}{\epsilon} - ik\right), \qquad (8)$$

where K is an effective shear modulus of the interface. The surface mechanical impedance can then be evaluated, taking

care to normalize to the area of shear waves in the QCM by including a factor a_c^2/a_e^2, where a_e is the radius of the active area (essentially the electrode area).

$$Z_L = \frac{a_c^2}{a_e^2} \frac{\sigma}{\partial u/\partial t}\bigg|_{r=0} \sim \frac{a_c^2}{z_e^2} \frac{K}{\omega \epsilon}(k\epsilon - i). \qquad (9)$$

Using Eqs. (4) and (5) we find

$$\Delta f = \frac{f_0}{\pi Z_q \omega a_e^2} \frac{K a_c^2}{\epsilon}, \qquad (10)$$

$$\Delta \Gamma = \frac{f_0}{\pi Z_q \omega a_e^2} K k a_c^2, \qquad (11)$$

and

$$\frac{\Delta \Gamma}{\Delta f} = k\epsilon. \qquad (12)$$

The interface is characterized by K, a_c, and ϵ. From a dimensional analysis, the quantity $K a_c^2/\epsilon$ defines a spring constant for the increased stiffness of the system and positive frequency shift. The increase in half bandwidth and dissipation due to sound propagation depends on the total contact area independent of the roughness. More importantly, we find that for interfaces where $\epsilon \sim$ constant, the frequency shift is proportional to the contact area while the loss tangent remains constant. On the other hand, in the limit of single-asperity interfaces where $\epsilon = a_c$, we recover the result of LJ, i.e., both the frequency shift and loss tangent are proportional to contact radius.

While LJ had no independent means of measuring the contact size, the data published in Ref. 17 allow one to determine whether the dependence of the frequency shift and loss tangent on the contact radius is self-consistent. For the smooth lubricated contact, Δf and $\Delta \Gamma/\Delta f$ are observed to increase with contact radius in the same fashion, agreeing with their model. In contrast, for rougher metal–metal contacts, Δf increases by at least a factor of 4 while $\Delta \Gamma/\Delta f$ remains essentially constant. This apparent departure from their model is explained within the roughness picture presented here.[38]

We may analyze the slopes of the data presented in Fig. 5 to show that our model gives reasonable results for the size and number of contacting regions. According to Eq. (10), for oscillations in the fundamental mode $\omega = 2\pi f_0$, the slope is given by

$$\frac{\Delta f}{A_c} = \frac{K}{2\pi^2 Z_q A_e \epsilon}, \qquad (13)$$

where $A_c = \pi a_c^2$, $A_e = 2.8 \times 10^{-5}$ m^2, and $Z_q = 8.8 \times 10^6$ kg m^{-2} s^{-1}. It is an approximation to consider only one value for the elasticity of the interface in our model, especially given the proposed spherical geometry of the wave fronts in the probe. Since the QCM response is correlated with the lateral deflection of the contact, one choice for K is the reduced shear modulus, G^*, of the interface:[39]

$$\frac{1}{G^*} = \frac{2 - \nu_1}{G_1} + \frac{2 - \nu_2}{G_2}. \qquad (14)$$

TABLE I. Calculation of contact region (asperity) radius for the W and silica probes.

Probe material	$\Delta f/A_c$ (from Fig. 5)	Asperity contact radius, ϵ
W tip ($R=12$ μm)	102 ± 1 Hz/μm^2	26 nm
Silica sphere ($R=0.5$ mm)	16.6 ± 0.3 Hz/μm^2	99 nm

Again, we consider the Ag film and quartz to be a single system, with shear modulus of 29 GPa, while the W tip and silica sphere have shear moduli of 135 GPa and 29 GPa, respectively. For the corresponding interfaces, the reduced shear moduli are then 13 and 8 GPa. Fitting Eq. (13) to the measured slopes in Fig. 5 allows us to estimate of the average size of asperity contacts, shown in Table I. These values are reasonable since asperities in this size range are commonly observed in STM images of QCM electrode surfaces (see, for example, Refs. 27 and 32). The range of areas displayed in Fig. 5 corresponds to a range of up to 330 nm in contact radius. Our data and model are both consistent with an interface involving a collection of distinct contact regions with a constant average size ϵ. Considering ϵ to be the radius of asperities, the number of asperity contacts may be estimated from the area ratio: $n = a_c^2/\epsilon^2$. For the W tip, we find the estimated number of asperity contacts varies from 1 to ~ 70 as contact area increases in Fig. 5. For the silica sphere, the number varies from 1 to ~ 10. Again, these values seem reasonable for our simple model. Presumably, one could determine the overall size of the contact zone by estimating the separation between contacts. However, this would require a more detailed analysis of the asperity height distribution and degree of deformation than the model justifies.

The model presented here indicates that changes in frequency shift are simply proportional to changes in local elasticity as long as the contact area and roughness remain unchanged. This clarifies the mechanism of lateral contrast in local elasticity imaging setups based on scanning probe–QCM combinations.[13–16] This model does not contradict the observation of *negative* frequency shifts in experiments with low modulus polymer probes on QCM surfaces.[20] One can show that the lower shear moduli and significantly larger contact areas imply that the wavelength of sound in the polymer is not larger than the contact radius, so the interaction is no longer in the near-field acoustic limit. In this case, theories based on plane waves apply, which predict the observed negative frequency shifts.[22] This might have been the case as well for the negative frequency shifts reported in Ref. 11 for tip–QCM interactions in the presence of water films.

The model we have described assumes the contact regions do not slip. Equation (8) shows that for a shear modulus of about 10 GPa, QCM oscillation amplitude $u_0 \sim 10$ nm (a typical value for the QCM's in these experiments),[27] and $\epsilon \sim 100$ nm, the shear stresses applied to the interface may extend into the GPa range, enough to cause significant plastic deformation and wear. Indeed, a transfer film was observed, apparently of silver from the electrode surface, on the silica sphere after the experiments. Indentation curves obtained with the QCM oscillating and static were compared, and it was found that the depth of penetration of the tip into

the oscillating QCM was nearly twice that of the static QCM, although both exhibited hysteresis. This suggests that in addition to elastoplastic deformation, wear was indeed occurring at some point during the indentations, implying fretting or slip. It is well known that the onset of slip depends on both oscillation amplitude and the load, with slip favored at larger amplitudes and smaller loads.[24] However, the results presented here are not sufficient to determine the degree of slip at the interfaces, and the model describes our data quite well in terms of no-slip boundary conditions.

Nevertheless, both mass-and-spring mechanical models and a recently published physical model[22] indicate that the onset of interfacial slip is associated with a decrease in the magnitude of the frequency shift and a broadening of the resonance due to frictional energy losses. These considerations indicate that it should be possible to investigate interfacial shear strengths, fretting, and high-speed sliding friction using probe–QCM techniques. The pressures and sliding speeds accessed would be relevant to the operation of microelectromechanical systems as well as macroscopic devices, for the former of which there historically have been very few nano- or microscale techniques operating in the appropriate physical regime.[40]

Finally, we see from our results that it should be possible to carry out nanomechanical studies with probe–QCM setups in which the number of contact regions is controllably varied over the mesoscopic range from a single to hundreds of contacts. Such studies would benefit greatly from specially prepared probe and/or substrate surfaces (with desirable morphologies or material properties), increased frequency shift sensitivity, and a wide variation of the QCM vibrational amplitude, for the possibility of studying both nonsliding and sliding contacts.

V. CONCLUSIONS

We have investigated the contact mechanics occurring at the interface between a probe tip and QCM surface. For the tip–surface combinations chosen, the data and modeling presented are consistent with an interface involving many discrete contact regions. The change in resonant frequency of the QCM is directly proportional to the contact area and reflects the elasticity of the interface and the number and average size of contact regions.

ACKNOWLEDGMENTS

[1] J. B. Pethica and D. Tabor, Surf. Sci. **89**, 182 (1979).

[2] J. B. Pethica and W. C. Oliver, Phys. Scr., T **19**, 61 (1987).

[3] N. A. Burnham and R. J. Colton, J. Vac. Sci. Technol. A **7**, 2906 (1989).

[4] N. A. Burnham, D. D. Dominguez, R. L. Mowery, and R. J. Colton, Phys. Rev. Lett. **64**, 1931 (1990).

[5] C. M. Mate, G. M. McClelland, R. Erlandsson, and S. Chiang, Phys. Rev. Lett. **59**, 1942 (1987).

[6] S. P. Jarvis, A. Oral, T. P. Weihs, and J. B. Pethica, Rev. Sci. Instrum. **64**, 3515 (1993).

[7] M. A. Lantz, S. O'Shea, M. E. Welland, and K. L. Johnson, Phys. Rev. B **55**, 10776 (1997).

[8] R. W. Carpick, D. F. Ogletree, and M. Salmeron, Appl. Phys. Lett. **70**, 1548 (1997).

[9] U. Dürig, O. Zuger, B. Michel, L. Haussling, and H. Ringsdorf, Phys. Rev. B **48**, 1711 (1993).

[10] G. Rubio, N. Agraït, and S. Vieira, Phys. Rev. Lett. **76**, 2302 (1996).

[11] J. Krim, A. Dayo, and C. Daly, *Atomic Force Microscopy/Scanning Tunneling Microscopy*, edited by S. H. Cohen *et al.* (Plenum, New York, 1994), p. 211.

[12] J. Krim, A. Dayo, and C. Daly, *Atomic Force Microscopy/Scanning Tunneling Microscopy*, edited by S. H. Cohen *et al.* (Plenum, New York, 1994), p. 303.

[13] A. Sasaki, A. Katsumata, F. Iwata, and H. Aoyama, Appl. Phys. Lett. **64**, 124 (1994).

[14] A. Sasaki, A. Katsumata, F. Iwata, and H. Aoyama, Jpn. J. Appl. Phys., Part 2 **33**, L547 (1994).

[15] R. Yamada, S. Ye, and K. Uosaki, Jpn. J. Appl. Phys., Part 2 **35**, L846 (1996).

[16] J. M. Kim and S. M. Chang, Appl. Phys. Lett. **74**, 466 (1999).

[17] A. Laschitsch and D. Johannsmann, J. Appl. Phys. **85**, 3759 (1999).

[18] A. Laschitsch, thesis (Logos Verlag, Berlin, 2000).

[19] A. Laschitsch, L. E. Bailey, G.W. Tyndall, C. W. Frank, and D. Johannsmann, Appl. Phys. Lett. **78**, 2601 (2001).

[20] C. M. Flanigan, M. Desai, and K. Shull, Langmuir **16**, 9825 (2000).

[21] G. L. Dybwad, J. Appl. Phys. **58**, 2789 (1985).

[22] G. McHale, R. Lucklum, M. I. Newton, and J. A. Cowen, J. Appl. Phys. **88**, 7304 (2000).

[23] S. A. Syed Asif, K. J. Wahl, and R. J. Colton, Rev. Sci. Instrum. **70**, 2408 (1999).

[24] K. L. Johnson, *Contact Mechanics* (Cambridge University Press, Cambridge, UK, 1985), p. 92.

[25] M. E. Frerking, *Crystal Oscillator Design and Temperature Compensation* (Van Nostrand Reinhold, New York, 1978), p. 85.

[26] The present experiment did not allow for the calibrated tracking of changes in energy dissipation via shifts in resonant amplitude, quality factor, or bandwidth of the QCM. Qualitatively, when large enough to be observable, the amplitude changes were negative, indicating increased energy dissipation.

[27] B. Borovsky, B. L. Mason, and J. Krim, J. Appl. Phys. **88**, 4017 (2000).

[28] S. A. Syed Asif, K. J. Wahl, and R. J. Colton, J. Mater. Res. **15**, 546 (2000).

[29] Indentations to 500 μN on the sacrificed QCM after the experiments indicated that under these conditions, the Ag film, and not the quartz substrate, dominated the mechanical response.

[30] W. C. Oliver and G. M. Pharr, J. Mater. Res. **7**, 1564 (1992).

[31] J. A. Greenwood, in *Fundamentals of Friction: Macroscopic and Microscopic Processes,* NATO ASI Series, edited by I. L. Singer and H. M. Pollock (Kluwer, Boston, 1992), p. 37.

[32] G. Palasantzas and J. Krim, Phys. Rev. Lett. **73**, 3564 (1994).

[33] R. Cernosek, S. Martin, A. R. Hillman, and H. Bandey, IEEE Trans. on Ultrasonics, Ferroelectrics and Frequency Control **45**, 1399 (1998).

[34] E. Benes, M. Schmid, and V. Kravchenko, J. Acoust. Soc. Am. **90**, 700 (1991).

[35] B. A. Martin and H. E. Hager, J. Appl. Phys. **65**, 2630 (1989).

[36] A. L. Fetter and J. D. Walecka, *Theoretical Mechanics of Particles and Continua* (McGraw-Hill, New York, 1980), p. 473.

[37] For instance, one can show these results hold for a rough-on-flat geometry given a Gaussian distribution of asperity heights. See Ref. 31. Such a distribution is commonly derived from STM images of the electrode surface.

[38] Information on measured surface roughness is presented by LJ in Ref. 18. The root-mean-square roughness for lubricated contact was about 0.25 nm, and for metal–metal contacts about 10 nm.

[39] K. L. Johnson, *Contact Mechanics* (Cambridge University Press, Cambridge, 1985), p. 217.

[40] I. L. Singer, J. Vac. Sci. Technol. A **12**, 2605 (1994).